GEOPHYSICAL RESEARCH LETTERS, VOL. 36, L05105, doi:10.1029/2008GL036803, 2009

Sheared flows and small-scale Alfvén wave generation in the auroral acceleration region

K. Asamura,[1] C. C. Chaston,[2] Y. Itoh,[1,3] M. Fujimoto,[1] T. Sakanoi,[4]
Y. Ebihara,[5] A. Yamazaki,[1] M. Hirahara,[3] K. Seki,[6] Y. Kasaba,[4] and M. Okada[7]

Received 26 November 2008; revised 21 January 2009; accepted 11 February 2009; published 11 March 2009.

[1] Coincident particle and optical measurements from the Reimei spacecraft suggest that sheared flows through an inverted-V arc may be unstable to the emission of Alfvén waves. The particle measurements reveal time dispersed field-aligned electron bursts typical of low energy electrons accelerated by inertial Alfvén waves (IAWs). These Alfvén wave accelerated electrons are embedded within multi-keV inverted-V electron structures. The optical measurements at the footprint of the inverted-V structures reveal counter propagating and folded/vortical discrete auroral forms moving with speeds of ~14–18 km/s. We show that the flow shear inferred from this motion exceeds that required for instability to the emission of Alfvén waves on scales of the order of an electron inertial length. The emission of these waves provides a likely means for driving the low energy dispersed electron bursts we observe. **Citation:** Asamura, K., et al. (2009), Sheared flows and small-scale Alfvén wave generation in the auroral acceleration region, *Geophys. Res. Lett.*, *36*, L05105, doi:10.1029/2008GL036803.

1. Introduction

[2] A number of studies have speculated that shear Alfvén waves on transverse scales of the order of an electron inertial length (λ_e) may drive fine-scale (~1 km) auroral features [e.g., *Goertz*, 1984]. On these scales shear Alfvén waves are often called inertial Alfvén waves (IAWs) and provide a feasible mechanism for field-aligned, small-scale electron acceleration at altitudes of a few thousand kilometers above the aurora [*Hasegawa*, 1976; *Goertz and Boswell*, 1979; *Goertz*, 1984; *Stasiewicz et al.*, 2000; *Chaston et al.*, 2002; *Lysak and Song*, 2003]. *Kletzing* [1994] showed IAWs could accelerate background electrons up to twice of local Alfvén velocity (with inertial correction) in the field-aligned direction. Plasma observations and numerical simulations confirm that downward energy fluxes of electrons accelerated by IAWs can reach sufficient levels to excite visible aurorae [*Chaston et al.*, 2003]. Despite these successes however, significant challenges in developing a self-consistent understanding of the operation of this process remain [e.g., *Stasiewicz et al.*, 2000; *Lysak and Song*, 2003; *Watt et al.*, 2005; *Seyler and Liu*, 2007].

[3] Travelling IAWs accelerate electrons through a resonant interaction with the field-aligned electric field ($E_\parallel$) carried by the wave. The efficient operation of this process requires significant spectral energy densities at $k_\perp \lambda_e \sim 1$ where $k_\perp$ is the wavenumber perpendicular to the geomagnetic field B_0. Hence the efficacy of the acceleration process is density dependent. Observations and Vlasov solutions [*Ergun et al.*, 2000] for density and potential distributions along geomagnetic field-lines through the auroral acceleration region reveal an abrupt interface between the tenuous plasmas of the magnetosphere and the much more dense plasmas of topside ionosphere. This interface, which delineates the base of the auroral acceleration region, occurs typically at altitudes above ~3000 km. At altitudes below this the efficiency of electron acceleration in IAWs is significantly reduced since $k_\perp \lambda_e \sim 1$ is shifted to larger wavenumbers with smaller spectral energy density. Consequently, this interface approximately defines the source altitude for electron energy-time dispersion often observed from sounding rockets and spacecraft [e.g., *McFadden et al.*, 1987; *Kletzing and Torbert*, 1994; *Clemmons et al.*, 1994; *Semeter et al.*, 2001; *Tanaka et al.*, 2005a]. The typical time scale of the dispersion is ~1 s or less and has been convincingly modelled using fluid simulations of Alfvén wave propagation and test particle electrons [*Kletzing and Hu*, 2001; *Chen et al.*, 2005; *Tanaka et al.*, 2005b].

[4] Despite the large number of in-situ observations of field-aligned dispersed electrons and Alfvén waves, there remains a scarcity of conjunctive optical and in-situ plasma measurements which identify a one-to-one correlation between specific auroral features and Alfvén wave accelerated electrons. This is due to the difficulty of unambiguously matching kilometer scale optical features at ~100 km altitude with plasma measurements from rapidly transiting spacecraft at much higher altitudes and the rareness of such close conjunctions. However, *Hallinan et al.* [2001] reported a transient tall rayed arc associated with lower energy electrons (less than ~1 keV) spreading in energy where Alfvén waves were identified with electric and magnetic field measurements, based on sounding rocket and ground-based observations. Also *Semeter and Blixt* [2006] found a time-dependent auroral arc structure which could be explained through IAW acceleration by assuming that the structure represented the projection of the IAW $E_\parallel$ into the $B_{0\perp}$ plane.

[5] In this paper, we present a case study of fine-scale auroral arc structures driven by inverted-V electrons and embedded dispersive electron bursts observed from the Reimei spacecraft. This spacecraft flies in a roughly polar

[1]ISAS, JAXA, Sagahamihara, Japan.
[2]Space Science Laboratory, University of California, Berkeley, California, USA.
[3]Graduate School of Science, University of Tokyo, Tokyo, Japan.
[4]Graduate School of Science, Tohoku University, Sendai, Japan.
[5]Institute for Advanced Research, Nagoya University, Nagoya, Japan.
[6]Solar-Terrestrial Environment Laboratory, Nagoya University, Nagoya, Japan.
[7]National Institute of Polar Research, Tokyo, Japan.

0094-8276/09/2008GL036803$05.00

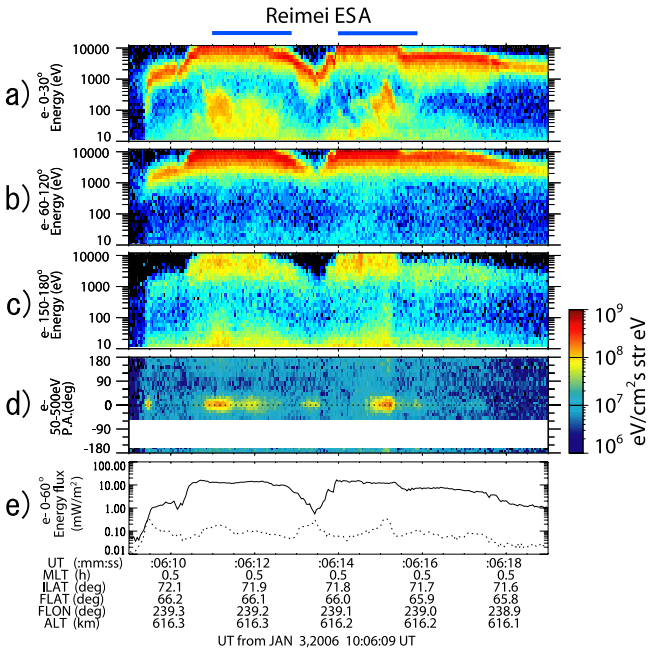

Figure 1. Observed electron energy fluxes of electrons in (a) precipitating, (b) perpendicular, and (c) upgoing directions. (d) Pitch angle distributions. (e) Electron energy fluxes in precipitating direction. Solid and dotted lines show the energy fluxes with energy ranges of 1–12 keV and 0.01–1 keV, respectively. Blue horizontal lines show time periods when sequences of auroral images presented in Figure 2 are taken.

circular orbit at an altitude of ~650 km and is equipped with high-time resolution particle analyzers and auroral cameras. These instruments allow us to simultaneously observe both particle energy spectra with full pitch-angle coverage, and auroral images in which the geomagnetic footprint of the spacecraft is captured, through the implementation of attitude control of the spacecraft. The high time resolution particle measurements combined with the high temporal and spatial resolution of the optical measurements allow unambiguous study of the spatial/temporal evolution of small scale auroral forms and the electron distributions which drive them.

2. Instrumentation

[6] The Reimei spacecraft carries electron/ion electrostatic energy analyzers and auroral imagers. Time resolutions are 40 ms and 120 ms for the particle energy spectra and the auroral images, respectively. Measured wavelengths of the imager are 670 nm, 557.7 nm, and 427.8 nm, which are filtered and detected separately. Detailed specifications of the instruments are described in other papers [*Asamura et al.*, 2003; *Sakanoi et al.*, 2003; *Obuchi et al.*, 2008]. Unfortunately, no scientific instruments measuring electric and magnetic fields are onboard Reimei spacecraft, although pitch angles of measured particles are deduced with an attitude magnetometer.

[7] In order to get the conjunction observations, locations of the geomagnetic footprints for every spacecraft positions are calculated. An altitude of the geomagnetic footprint is set to be 110 km, since the onboard auroral imagers measure emissions typically coming from the ionospheric E-region. Then the footprint locations are numerically calculated by field-line tracings from spacecraft location to the footprint altitude. The geomagnetic field is given by the IGRF-10 model.

3. Observation

[8] Reimei spacecraft made the particle – auroral image simultaneous measurement in the midnight auroral oval at 10:05:43–10:06:42 UT, Jan. 3, 2006. Figure 1 shows measured differential energy fluxes of electrons between 10:06:09 and 10:06:19 UT. Figures 1a, 1b, and 1c show the energy fluxes of precipitating (pitch angles of 0°–30°), perpendicular (60°–120°), and upgoing (150°–180°) electrons, respectively. Figure 1d shows corresponding pitch angle distributions with an energy range from 50 to 500 eV. Note that the perpendicular fluxes with energies less than ~50 eV are affected by instrumental effects significantly. There are two inverted-V structures which are continuously located, 10:06:09.5–10:06:13.5 UT and 10:06:13.5–10:06:28 UT (latter half is not shown). Both inverted-V structures are colocated with precipitating beams whose energies are lower than those of the inverted-Vs at time periods of 10:06:10.5–10:06:12.5 UT and 10:06:14.0–10:06:15.5 UT. These low-energy precipitating beams are time-dispersed, and confined with pitch angles less than 30°. Figure 1e shows electron energy fluxes in precipitating direction (pitch angles of 0°–60°). Note that half of loss cone angle is ~60°. Solid and dotted lines show the energy fluxes with energy ranges of 1–12 keV and 0.01–1 keV, respectively. They primarily correspond to the inverted-V structures and the low-energy beams, respectively, at the time periods when the low-energy precipitating beams appear. Most of precipitating electron energy flux is contained in the inverted-V electrons.

[9] Figure 2 shows observed image sequences of auroral emissions with a wavelength of 670 nm at time periods when the low-energy precipitating beams appear in the electron data. The sequence periods are 10:06:11.0–10:06:12.9 UT and 10:06:14.0–10:06:15.9 UT, which are also indicated as blue horizontal lines in Figure 1. Yellow cross marks and dotted lines on the images indicate the geomagnetic footprints corresponding to the spacecraft locations and trajectories, respectively (i.e., locations of the electron measurements). There are four distinct arcs, labelled A, B, C, and D from poleward to equatorward. These arcs contain fine structures as curls and folds with typical spatial scales of ~5–10 km. The fine structures in arc C are moving eastward, and those of arc D are moving westward, as shown by white arrows schematically in Figure 2. The same feature also appear for arcs A and B, although they are connected by a hairpin turn (large-scale fold) in the lefthand (west) side of the image. At the hairpin turn, the fine structures move clockwise, forming a continuous flow from arc B to arc A. Flow velocities of fine structures in arcs A, B, C, and D are 14 (eastward), 17 (westward), 15 (eastward), and 18 km/s (westward) on the average in a reference frame of the earth (rotating), respectively, where the velocities are calculated with a minimum

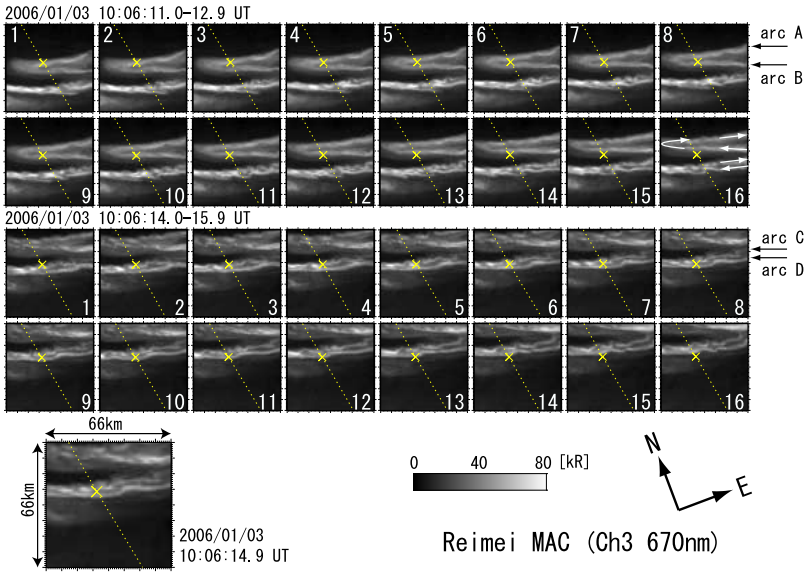

Figure 2. Image sequences of auroral emissions with a wavelength of 670 nm at time periods when the precipitating beams of low-energy electrons appear. An image on the lower left is magnified one for 2006/01/03 10:06:14.9 UT (sequence number 8). Yellow cross marks and dotted lines indicate the geomagnetic footprints corresponding to the spacecraft locations and trajectories, respectively. White arrows on the image schematically indicate flow directions of auroral fine structures. Directions shown at the lower right indicate geomagnetic north and east. Equator is located at southward.

mean square error analysis described by *Ebihara et al.* [2007].

4. Discussion and Conclusion

[10] The plasma measurements reveal two distinct electron populations often identified from spacecraft traversing high-latitude fieldlines above discrete auroral arcs. Since auroral emission intensity is roughly proportional to the precipitating electron energy flux, Figure 1e demonstrates that the inverted-V electron population is responsible for the auroral luminosity shown in Figure 2. The lower energy time-dispersed population while not contributing significantly to the auroral luminosity, provides a useful diagnostic for examining processes in the region where the inverted-V electron acceleration is occurring. These electrons have the properties of electrons accelerated in IAWs (see section 1) including (1) field-aligned pitch-angle distributions, (2) time-dispersion on scales of ~0.5 s, and (3) energies less than the mono-energetic peak of the inverted-V. The presence of these 'Alfvénic' electrons embedded within the inverted-V is indicative of a process whereby the accelerating potential structure may be unstable to the emission of IAWs.

[11] A possible free energy source for this instability is suggested by the correlation of the 'Alfvénic' electrons with the camera observations of counterstreaming auroral forms. These forms travel eastward and westward on the poleward (arcs A and C) and equatorward arcs (arcs B and D) shown in Figure 2. It has previously been demonstrated that these counterstreaming features arise naturally from flow shears due to E × B drift [*Hallinan and Davis*, 1970] in the converging electric field structures known to bracket inverted-V electron structures above aurora [*Temerin et al.*, 1981]. Instabilities in the sheared flows are thought to account for the formation of the small scale arc-aligned (azimuthal) folds and curls visible in these images and have been documented previously [*Hallinan and Davis*, 1970; *Davis*, 1978; *Haerendel et al.*, 1996]. The correlation between 'Alfvénic' electrons and flow shear we report here however, suggest that in addition to driving the well known azimuthal structuring of auroral forms, instabilities in these sheared flows may drive the emission of IAWs.

[12] The generation of shear Alfvén waves through velocity shear in the auroral acceleration region has been predicted from theory by *Peñano and Ganguli* [2000] and *Wu and Seyler* [2003]. The instability involves the resonant interaction of the wave with the flow given by $\omega - k_y V_y(x) = 0$ where ω is the wave angular frequency, k_y the azimuthal wavenumber and $V_y(x)$ the azimuthal flow speed at the location of the resonance. A necessary threshold criterion for this instability is given by *Wu and Seyler* [2003] as $(\omega_s/\Omega_i)(k_y/k_z) > 2$ where $\omega_s = \partial V_y/\partial x$ is the shear frequency, and Ω_i, and k_z are the ion cyclotron frequency, and wavenumber along the geomagnetic field direction respectively. In addition to satisfying this condition, significant wave growth requires multiple interactions of the wave with the flow. This may be provided by wave reflection from transverse density gradients present on the edges of auroral acceleration regions [*Ergun et al.*, 1998] or by reflections from the ionosphere [*Lysak*, 1991]. The required observables to determine the range of unstable wavenumbers for our case study example include the local geomagnetic field strength where the instability occurs and the magnitude of the flow shear at the same altitude. Both of these can be estimated from Reimei observations as we now detail.

[13] The altitude of the lower boundary of the auroral acceleration region can be estimated, as described in the introduction, from the energy dependent arrival times of the 'Alfvénic' electrons. An altitude of ~3000 km on the

average is estimated by performing this analysis for the dispersed electrons measured at 10:06:10.83–11.11 UT, 10:06:14.83–15.11 UT, and 10:06:15.11–15.31 UT, which is consistent with FAST spacecraft observations [*Paschmann et al.*, 2002]. ω_s can then be estimated from the motion of the auroral forms under the assumption that the cross-field displacement of the inverted-V electrons through the regions of $E_{\parallel}$ is less than the E × B drift they experience above and through the acceleration region. We acknowledge that there is some uncertainty as to the validity of this assumption and refer to the arguments given by *Hallinan* [1981, p. 46] in support of its use. Mapping the observed azimuthal flow speeds up the geomagnetic field from 110 km to 3000 km altitude yields speeds of $V_y \sim 30$ km/s. At 3000 km altitude an E × B drift speed of this size requires an electric field of $E_x \sim 5 \times 10^2$ mV/m. Such field strengths are often observed by spacecraft traversing the auroral acceleration region [*Ergun et al.*, 1998]. The optical measurements shown in Figure 2, indicate widths across each auroral arc system of ~5–10 km with the finer scale counterstreaming elements on ~1 km scales similar to expected values for λ_e in the acceleration region. The gradients in the observed flows therefore provide $\omega_s/\Omega_{H^+} \approx 0.01$ and $\omega_s/\Omega_{O^+} \approx 0.17$ at 3000 km altitude. Consequently the flows may be unstable to IAWs at this altitude with $k_y/k_z > 190$ and 12 for H^+ and O^+ ions, respectively. The ion plasma at 3000 km altitude in the auroral region may contain a significant fraction of O^+ and so the appropriate threshold will be intermediate between these two values. We also note that since the ratio ω_s/Ω_{H^+} scales with $1/B_0$ the unstable wavenumber range will increase with altitude above 3000 km to include less oblique angles of propagation. For this reason the unstable range we identify at 3000 km altitude represents a conservative estimate of the likely unstable range. Nonetheless, this range is consistent with the observations of IAWs from the Freja [*Wahlund et al.*, 1998] and FAST [*Chaston et al.*, 2006] spacecraft where interferometric measurements have revealed wavevectors nearly perpendicular to B_0. These estimates therefore provide a plausible argument for the emission of IAWs from sheared flows in the auroral acceleration region.

[14] Resonance with the flow for Alfvén wavelengths along the arc similar to the spatial periodicity of folds/curls observed in the counterstreaming forms (~8 km) defines a range of wave frequencies of ~1 Hz and less. Significantly this range includes the resonant frequencies of the ionospheric Alfvén resonator (IAR) [*Lysak*, 1991]. The trapping of these waves between the ionosphere and the auroral acceleration region within the IAR provides a means to pump-up wave amplitude through repeated resonant interaction with the flow. This is in addition to the possible wave growth driven by the feedback response of the ionosphere [*Lysak and Song*, 2002]. We suggest that this combined interaction may provide IAW amplitudes sufficient to drive electron acceleration and account for the low energy dispersive electron fluxes we observe coincident with the inverted-V electrons and the counterstreaming auroral forms.

[15] **Acknowledgments.** The authors thank the development and operation team of Reimei (former INDEX) spacecraft. A part of Reimei tracking is supported by National Institute of Polar Research, Japan, with Syowa Station in Antarctica. The work of Y. E. is supported by the Program for Improvement of Research Environment for Young Researchers from the Special Coordination Funds for Promoting Science and Technology (SCF) commissioned by the Ministry of Education, Culture, Sports, Science and Technology (MEXT) of Japan. This study is also supported by Grant-in-Aid for Scientific Research (B) (19340141) by Japan Society for the Promotion of Science (JSPS).

References

Asamura, K., et al. (2003), Auroral particle instrument onboard the index satellite, *Adv. Space Res.*, *32*, 375.

Chaston, C. C., J. W. Bonnell, L. M. Peticolas, C. W. Carlson, J. P. McFadden, and R. E. Ergun (2002), Driven Alfven waves and electron acceleration: A FAST case study, *Geophys. Res. Lett.*, *29*(11), 1535, doi:10.1029/2001GL013842.

Chaston, C. C., L. M. Peticolas, J. W. Bonnell, C. W. Carlson, R. E. Ergun, J. P. McFadden, and R. J. Strangeway (2003), Width and brightness of auroral arcs driven by inertial Alfven waves, *J. Geophys. Res.*, *108*(A2), 1091, doi:10.1029/2001JA007537.

Chaston, C. C., V. Genot, J. W. Bonnell, C. W. Carlson, J. P. McFadden, R. E. Ergun, R. J. Strangeway, E. J. Lund, and K. J. Hwang (2006), Ionospheric erosion by Alfven waves, *J. Geophys. Res.*, *111*, A03206, doi:10.1029/2005JA011367.

Chen, L.-J., C. A. Kletzing, S. Hu, and S. R. Bounds (2005), Auroral electron dispersion below inverted-V energies: Resonant deceleration and acceleration by Alfven waves, *J. Geophys. Res.*, *110*, A10S13, doi:10.1029/2005JA011168.

Clemmons, J. H., M. H. Boehm, G. E. Paschmann, and G. Haerendel (1994), Signature of energy-time dispersed electron fluxes measured by Freja, *Geophys. Res. Lett.*, *21*, 1899.

Davis, T. N. (1978), Observed characteristics of auroral arcs, *Space Sci. Rev.*, *22*, 77.

Ebihara, Y., Y.-M. Tanaka, S. Takasaki, A. T. Weatherwax, and M. Taguchi (2007), Quasi-stationary auroral patches observed at the South Pole Station, *J. Geophys. Res.*, *112*, A01201, doi:10.1029/2006JA012087.

Ergun, R. E., et al. (1998), FAST satellite observations of electric field structures in the auroral zone, *Geophys. Res. Lett.*, *25*, 2061.

Ergun, R. E., C. W. Carlson, J. P. McFadden, F. S. Mozer, and R. J. Strangeway (2000), Parallel Electric Fields in Discrete Arcs, *Geophys. Res. Lett.*, *27*, 4053–4056.

Goertz, G. K. (1984), Kinetic Alfvén waves on auroral field lines, *Planet. Space Sci.*, *32*, 1387.

Goertz, G. K., and R. W. Boswell (1979), Magnetosphere-ionosphere coupling, *J. Geophys. Res.*, *84*, 7239.

Haerendel, G., et al. (1996), Optical and radar observations of auroral arcs with emphasis on small-scale structures, *J. Atmos. Terr. Phys.*, *58*, 71.

Hallinan, T. J. (1981), The distribution of vorticity in auroral arcs, in *Physics of Auroral Arc Formation*, *Geophys. Monogr. Ser.*, *25*, edited by S.-I. Akasofu and J. R. Kan, p. 42, AGU, Washington, D. C.

Hallinan, T. J., and T. N. Davis (1970), Small-scale auroral arc distortions, *Planet. Space Sci.*, *18*, 1735.

Hallinan, T. J., et al. (2001), Relation between optical emissions, particles, electric fields, and Alfvén waves in a multiple rayed arc, *J. Geophys. Res.*, *106*, 15,445.

Hasegawa, A. (1976), Particle acceleration by MHD surface wave and formation of aurora, *J. Geophys. Res.*, *81*, 5083.

Kletzing, C. A. (1994), Electron acceleration by kinetic Alfvén waves, *J. Geophys. Res.*, *99*, 11,905.

Kletzing, C. A., and S. Hu (2001), Alfvén wave generated electron time dispersion, *Geophys. Res. Lett.*, *28*, 693.

Kletzing, C. A., and R. B. Torbert (1994), Electron time dispersion, *J. Geophys. Res.*, *99*, 2159.

Lysak, R. L. (1991), Feedback instability of the ionospheric resonant cavity, *J. Geophys. Res.*, *96*, 1553.

Lysak, R. L., and Y. Song (2002), Energetics of the ionospheric feedback interaction, *J. Geophys. Res.*, *107*(A8), 1160, doi:10.1029/2001JA000308.

Lysak, R. L., and Y. Song (2003), Kinetic theory of the Alfvén wave acceleration of auroral electrons, *J. Geophys. Res.*, *108*(A4), 8005, doi:10.1029/2002JA009406.

McFadden, J. P., C. W. Carlson, and M. H. Boehm (1987), Field-aligned electron flux oscillations that produce flickering aurora, *J. Geophys. Res.*, *92*, 11,133.

Obuchi, Y., et al. (2008), Initial observations of auroras by the multispectral auroral camera on board the Reimei satellite, *Earth Planet. Space*, *60*, 827.

Paschmann, G., S. Haaland, and R. Treumann (2002), Auroral plasma physics, *Space Sci. Rev.*, *103*, 1.

Peñano, J. R., and G. Ganguli (2000), Generation of ELF electromagnetic waves in the ionosphere by localized transverse dc electric fields: Subcyclotron frequency regime, *J. Geophys. Res.*, *105*, 7441.

Sakanoi, T., et al. (2003), Development of the multi-spectral auroral camera onboard the index satellite, *Adv. Space Res.*, *32*, 379.

Semeter, J., and E. M. Blixt (2006), Evidence for Alfvén wave dispersion identified in high-resolution auroral imagery, *Geophys. Res. Lett.*, *33*, L13106, doi:10.1029/2006GL026274.

Semeter, J., J. Vogt, and G. Haerendel (2001), Persistent quasiperiodic precipitation of suprathermal ambient electrons in decaying auroral arcs, *J. Geophys. Res.*, *106*, 12,863.

Seyler, C. E., and K. Liu (2007), Particle energization by oblique inertial Alfvén waves in the auroral region, *J. Geophys. Res.*, *112*, A09302, doi:10.1029/2007JA012412.

Stasiewicz, K., et al. (2000), Small scale Alfvénic structure in the aurora, *Space Sci. Rev.*, *92*, 423.

Tanaka, H., Y. Saito, K. Asamura, S. Ishii, and T. Mukai (2005a), High time resolution measurement of multiple electron precipitations with energy-time dispersion in high-latitude part of the cusp region, *J. Geophys. Res.*, *110*, A07204, doi:10.1029/2004JA010664.

Tanaka, H., Y. Saito, K. Asamura, and T. Mukai (2005b), Numerical modeling of electron energy-time dispersions in the high-latitude part of the cusp region, *J. Geophys. Res.*, *110*, A05213, doi:10.1029/2004JA010665.

Temerin, M., M. H. Boehm, and F. S. Mozer (1981), Paired electrostatic shocks, *Geophys. Res. Lett.*, *8*, 799.

Wahlund, J.-E., et al. (1998), Broadband ELF plasma emission during auroral energization: 1. Slow ion acoustic waves, *J. Geophys. Res.*, *103*, 4343.

Watt, C. E. J., R. Rankin, I. J. Rae, and D. M. Wright (2005), Self-consistent electron acceleration due to inertial Alfvén waves, *J. Geophys. Res.*, *110*, A10S07, doi:10.1029/2004JA010877.

Wu, K., and C. E. Seyler (2003), Instability of inertial Alfvén waves in transverse sheared flow, *J. Geophys. Res.*, *108*(A6), 1236, doi:10.1029/2002JA009631.

K. Asamura, M. Fujimoto, Y. Itoh and A. Yamazaki, Institute of Space and Astronautical Science, JAXA, Sagamihara 229-8510, Japan. (asamura@stp.isas.jaxa.jp)

C. C. Chaston, Space Science Laboratory, University of California, Berkeley, CA 94720, USA.

Y. Ebihara, Institute for Advanced Research, Nagoya University, Nagoya 464-8601, Japan.

M. Hirahara, Graduate School of Science, University of Tokyo, Tokyo 113-0033, Japan.

Y. Kasaba and T. Sakanoi, Graduate School of Science, Tohoku University, Sendai 980-8578, Japan.

M. Okada, National Institute of Polar Research, Tokyo 173-8515, Japan.

K. Seki, Solar-Terrestrial Environment Laboratory, Nagoya University, Nagoya 464-8601, Japan.